

MHyper: Multi-Scale Hypergraph Transformer for Long-Range Time Series Forecasting

Zongjiang Shang¹, Ling Chen¹*

¹College of Computer Science and Technology, Zhejiang University, Hangzhou 310027, China
{zongjiangshang, lingchen}@cs.zju.edu.cn

Abstract

Demystifying interactions between temporal patterns of different scales is fundamental to precise long-range time series forecasting. However, previous works lack the ability to model high-order interactions. To promote more comprehensive pattern interaction modeling for long-range time series forecasting, we propose a **M**ulti-**S**cale **H**ypergraph Transformer (MHyper) framework. Specifically, a multi-scale hypergraph is introduced to provide foundations for modeling high-order pattern interactions. Then by treating hyperedges as nodes, we also build a hyperedge graph to enhance hypergraph modeling. In addition, a tri-stage message passing mechanism is introduced to aggregate pattern information and learn the interaction strength between temporal patterns of different scales. Extensive experiments on five real-world datasets demonstrate that MHyper achieves state-of-the-art performance, reducing prediction errors by an average of 8.73% and 7.15% over the best baseline in MSE and MAE, respectively.

1 Introduction

Many time series demonstrate complex and diverse temporal patterns of different scales [Wen *et al.*, 2021; Chen *et al.*, 2022; Chen *et al.*, 2023a; Zhang and Yan, 2023]. For example, due to periodic human activities, traffic occupation and electricity consumption show clear daily and weekly patterns. Considering interactions between these temporal patterns often leads to more accurate forecasting results than analyzing each pattern separately. For example, the morning rush hour on the first workday after a holiday tends to be more congested (interactions between daily and weekly patterns), while the evening rush hour on the last workday before a long holiday starts earlier. Therefore, how to model complex temporal patterns of different scales and their interactions is a fundamental problem in long-range time series forecasting.

To model temporal patterns of different scales and their interactions, traditional methods, e.g., seasonal ARIMA [Box and Jenkins, 1968] and Prophet [Taylor and Letham, 2018],

use decomposition with heuristic priors to obtain temporal patterns of different scales, but cannot model complex non-linear dependencies of time series. Recently, deep neural networks have demonstrated superiority in capturing non-stationary and non-linear dependencies. Temporal convolutional networks (TCNs) [Bai *et al.*, 2018], recurrent neural networks (RNNs) [Salinas *et al.*, 2020], and Transformers [Zhou *et al.*, 2021; Wu *et al.*, 2021] have been used for time series forecasting. To model temporal patterns of different scales, multi-scale Transformer-based methods [Li *et al.*, 2019] attempt to build sub-sequences of different scales from the original input sequence but ignore interactions between temporal patterns of different scales. To address this issue, recent multi-scale Transformer-based methods [Liu *et al.*, 2021; Cirstea *et al.*, 2022] introduce special structures (e.g., pyramidal structures) between sub-sequences of different scales. These structures model temporal dependencies within a sub-sequence through intra-scale edges, and model interactions between temporal patterns of different scales through inter-scale edges.

However, these methods only use edges to model pairwise interactions and lack the ability to model high-order interactions (i.e., simultaneous interactions between multiple temporal patterns). In reality, temporal patterns of different scales co-exist and exhibit high-order interactions, e.g., the peak household electricity consumption during summer weekend afternoons (high-order interactions between daily, weekly, and monthly patterns), as well as the high but relatively stable household electricity consumption during winter weekends.

To address the above issue, we propose MHyper, a **M**ulti-**S**cale **H**ypergraph Transformer framework for long-range time series forecasting. MHyper aggregates the input sequence into sub-sequences of different scales, and models high-order interactions between temporal patterns of different scales by building multi-scale hypergraph structures. To the best of our knowledge, MHyper is the first work that incorporates hypergraph modeling into long-range time series forecasting. The main contributions are as follows:

- 1) We propose a hypergraph and hyperedge graph construction (H-HGC) module that builds the hypergraph according to the temporal proximity rules, which can model intra-scale, inter-scale, and mixed-scale high-order interactions between temporal patterns. In addition, by treating hyperedges as nodes and building edges based on the sequential relation-

*Corresponding author.

ship and association relationship between nodes, H-HGC also builds the hyperedge graph to enhance hypergraph modeling.

2) We propose a tri-stage message passing (TMP) mechanism that has three message passing phases: Node-hyperedge, hyperedge-hyperedge, and hyperedge-node, which can aggregate pattern information and learn the interaction strength between temporal patterns of different scales.

3) We conduct extensive experiments on five real-world time series datasets, experimental results demonstrate that MSHyper achieves competitive performance, reducing prediction errors by an average of 8.73% and 7.15% over the best baseline in MSE and MAE, respectively.

2 Related Work

Methods for Time Series Forecasting. Time series forecasting methods can be roughly divided into statistical methods and deep neural network-based methods. Statistical methods (e.g., ARIMA [Box and Jenkins, 1968] and Prophet [Taylor and Letham, 2018]) follow arbitrary yet simple assumptions, and fail to model complicated temporal dependencies. Recently, deep neural networks show superiority in modeling complicated temporal dependencies. TAMS-RNNs [Chen *et al.*, 2021] obtains the periodic temporal dependencies through multi-scale recurrent neural networks (RNNs) with different update frequencies. LSTNet [Lai *et al.*, 2018] utilizes recurrent-skip connections in combination with convolutional neural networks (CNNs) to capture long- and short-term temporal dependencies. Transformer-based methods [Wen *et al.*, 2022; Chen *et al.*, 2023b] take advantage of the attention mechanism and achieve great access in modeling long-range temporal dependencies. Reformer [Kitaev *et al.*, 2020] approximates the attention value through local-sensitive hashing (LSH), Informer [Zhou *et al.*, 2021] obtains the dominant query by calculating the KL-divergence to realize the approximate of self-attention, and Autoformer [Wu *et al.*, 2021] introduces an auto-correlation mechanism to operate at the level of sub-sequences. However, the above methods struggle to obtain the complex temporal patterns of long-range time series.

Multi-Scale Transformers. Multi-scale or hierarchical Transformers have been proposed in different fields, e.g., natural language processing [Ainslie *et al.*, 2020; Guo *et al.*, 2019; Subramanian *et al.*, 2020], computer vision [Zhang *et al.*, 2021; Dosovitskiy *et al.*, 2021; Wang *et al.*, 2021], and time series forecasting [Chen *et al.*, 2022; Zhou *et al.*, 2022; Shabani *et al.*, 2022]. Multi-scale ViT [Zhang *et al.*, 2021] realizes image recognition by combining multi-scale image feature embeddings and Transformer. Star-Transformer [Guo *et al.*, 2019] models intra-scale and inter-scale information interactions by introducing the global node embedding. Due to the limited expression capacity of a single global node, ETC [Ainslie *et al.*, 2020] carries out information interactions between the global and local nodes by introducing a set of global node embeddings and setting fixed-length windows. To further extend the ability to model interactions between temporal patterns of different scales, Pyraformer [Liu *et al.*, 2021] extends the two-layer structure into multi-scale embeddings, and models interactions between nodes of different scales through a pyramid graph. Crossformer [Zhang

and Yan, 2023] combines a two-stage attention with a hierarchical encoder-decoder architecture to capture cross-time and cross-dimension interactions. However, existing methods only model pairwise interactions between nodes, ignoring high-order interactions between temporal patterns of different scales.

Hypergraph Neural Networks. Hypergraph neural networks (HGNNs) have been proven to be capable of modeling high-order interactions, which have been applied to various fields, e.g., visual object recognition [Yan *et al.*, 2020], trajectory prediction [Xu *et al.*, 2022], stock selection [Sawhney *et al.*, 2021], and citation network classification [Bai *et al.*, 2021]. HGNN [Feng *et al.*, 2019] and HyperGCN [Yadati *et al.*, 2019] are the first works to apply graph convolution to hypergraphs, which demonstrate the superiority of hypergraphs over ordinary graph neural networks (GNNs) in modeling high-order interactions. Recent works [Yang *et al.*, 2020; Xia *et al.*, 2022] show that HGNNs are promising to model pattern interactions from high-order relations. MBHT [Yang *et al.*, 2022] combines hypergraphs with a Transformer framework for the sequential recommendation, which leverages hypergraphs to capture high-order user-item interaction patterns. GroupNet [Xu *et al.*, 2022] uses multi-scale hypergraphs for trajectory prediction, which leverages topology inference and representation learning to capture the agent patterns with their high-order interactions.

Considering the ability of HGNNs in high-order interaction modeling, we propose a multi-scale hypergraph Transformer framework to model high-order interactions between temporal patterns of different scales. Specifically, a H-HGC module is introduced to build the hypergraph and hyperedge graph. In addition, a TMP mechanism is proposed to aggregate pattern information and learn the interaction strength between temporal patterns of different scales by three message passing phases.

3 Preliminaries

Hypergraph. A hypergraph is defined as $\mathcal{G} = \{\mathcal{V}, \mathcal{E}\}$, where $\mathcal{E} = \{e_1, e_2, \dots, e_M\}$ is the hyperedge set and $\mathcal{V} = \{v_1, v_2, \dots, v_N\}$ is the node set. Each hyperedge $e_m \in \mathcal{E}$ contains a set of nodes $\{v_1, v_2, \dots, v_n\} \subseteq \mathcal{V}$. The hypergraph \mathcal{G} can be denoted as an incidence matrix $\mathbf{H} \in \mathbb{R}^{N \times M}$, where $\mathbf{H}_{nm} = 1$ if the n th node belongs to the m th hyperedge, else $\mathbf{H}_{nm} = 0$. The degree of the n th node is defined as follows:

$$\mathbf{D}_{v_n} = \sum_{m=1}^M \mathbf{H}_{nm}. \quad (1)$$

The degree of the m th hyperedge is defined as follows:

$$\mathbf{D}_{e_m} = \sum_{n=1}^N \mathbf{H}_{nm}. \quad (2)$$

The results of node degrees and hyperedge degrees are stored in diagonal matrices $\mathbf{D}_v \in \mathbb{R}^{N \times N}$ and $\mathbf{D}_e \in \mathbb{R}^{M \times M}$, respectively.

Problem Statement. The task of long-range time series forecasting is to predict the future H steps given the previous

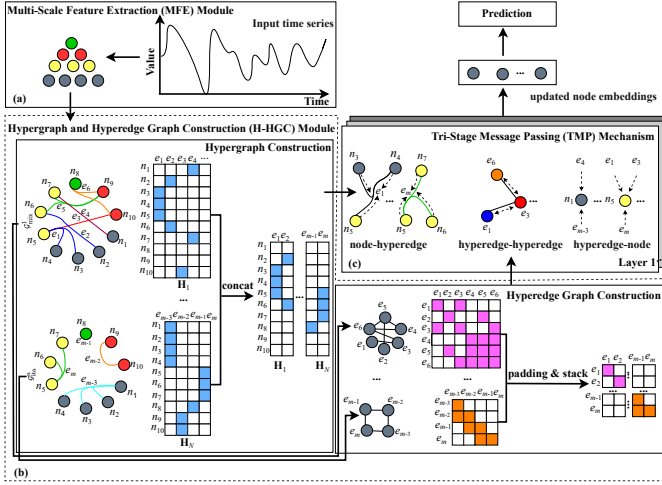


Figure 1: The framework of MSHyper, which consists of three parts: The multi-scale feature extraction (MFE) module, the hypergraph and hyperedge graph construction (H-HGC) module, and the tri-stage message passing (TMP) mechanism.

T steps of observed values. Specifically, given the input sequence $\mathbf{X}_{1:T}^1 = \{\mathbf{x}_t \mid \mathbf{x}_t \in \mathbb{R}^D, t \in [1, T]\}$, where \mathbf{x}_t represents the values at time step t , and D is the feature dimension. The prediction task can be formulated as:

$$\mathbf{X}_{T+1:T+H}^0 = \mathcal{F}(\mathbf{X}_{1:T}^1; \theta) \in \mathbb{R}^{H \times D}, \quad (3)$$

where $\mathbf{X}_{T+1:T+H}^0$ denotes the forecasting results, \mathcal{F} denotes the mapping function, and θ denotes the learnable parameters of \mathcal{F} .

4 MSHyper

As mentioned above, the core of MSHyper is to build multi-scale hypergraph structures, which can explicitly model high-order interactions between temporal patterns of different scales. To accomplish this goal, we first map the input sequence into multi-scale embeddings through the multi-scale feature extraction (MFE) module and then leverage the H-HGC module to build the hypergraph and hyperedge graph. Finally, we employ the TMP mechanism to aggregate pattern information and learn the interaction strength between temporal patterns of different scales. Figure 1 illustrates the framework of MSHyper.

4.1 Multi-Scale Feature Extraction Module

To get the feature embeddings of different scales, we first map the input sequence into multi-scale embeddings. Concretely, suppose $\mathbf{X}^s = \{\mathbf{x}_t^s \mid \mathbf{x}_t^s \in \mathbb{R}^D, t \in [1, h^s]\}$ denotes the sub-sequence at scale s , where $s = 1, \dots, S$ denotes the scale index, and S is the total number of scales. $h^s = \lfloor \frac{h^{s-1}}{l^{s-1}} \rfloor$ s.t. $s \geq 2$ is the horizon at scale s and l^{s-1} denotes the size of the aggregation window at scale $s-1$. $\mathbf{X}^1 = \mathbf{X}_{1:T}^1$ is the raw input sequence and the aggregation process can be formulated as:

$$\mathbf{X}^{s+1} = \text{Aggregation}(\mathbf{X}^s; \theta^s) \in \mathbb{R}^{h^{s+1} \times D}, \quad (4)$$

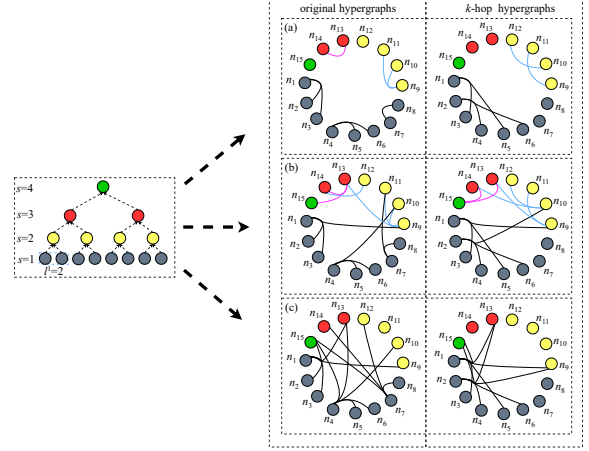


Figure 2: Hypergraph construction. (a), (b), and (c) represent the intra-scale hypergraph, inter-scale hypergraph, and mixed-scale hypergraph, respectively.

where *Aggregation* is the aggregation function, e.g., 1D convolution or average pooling, and θ^s denotes the learnable parameters of the aggregation function at scale s .

4.2 Hypergraph and Hyperedge Graph Construction Module

Hypergraph Construction

Despite existing methods [Liu *et al.*, 2021; Wu *et al.*, 2019] being capable of modeling interactions between temporal patterns of different scales through graph structures, we argue that these methods still face two limitations: (1) These methods fail to model high-order interactions between temporal patterns. (2) These methods limit interactions to the neighboring nodes and thus are incapable of capturing interactions between nodes that are far away but still show correlations. To address these problems, we build the hypergraph structures according to the temporal proximity rules. As shown in Figure 2, on the one hand, we build different types of hypergraphs to model intra-scale, inter-scale, and mixed-scale high-order interactions. On the other hand, we build the k -hop hypergraph under each type of hypergraph to aggregate information from different ranges of neighbors.

Intra-Scale Hypergraph. As shown in Figure 2(a), in order to capture high-order interactions between intra-scale temporal patterns, we construct the intra-scale hypergraph \mathcal{G}_{ita} , which contains two hypergraphs, i.e., the original intra-scale hypergraph $\mathcal{G}_{\text{o, ita}}$ and k -hop intra-scale hypergraph $\mathcal{G}_{\text{k, ita}}$. Mathematically, let $\mathcal{G}_{\text{o, ita}} = \{\mathcal{V}, \mathcal{E}_{\text{o, ita}}\}$ be the original intra-scale hypergraph, where $\mathcal{E}_{\text{o, ita}} = \{\mathcal{E}_{\text{o, ita}}^s \mid s \in \{1, \dots, S\}\}$ contains original intra-scale hyperedge sets of different scales. The i th hyperedge of scale s $e_i^s \in \mathcal{E}_{\text{o, ita}}^s$ is defined as follows:

$$e_i^s = \{v_\epsilon^s, \forall v_j^s \in \mathcal{N}(v_\epsilon^s)\} \text{ s.t. } 0 < j - \epsilon \leq H_s, \quad (5)$$

where $\epsilon = (i-1)H_s + 1$ is the starting node index under the i th hyperedge of scale s based on original connections. H_s is the number of nodes connected by each hyperedge of scale s and $\mathcal{N}(v_\epsilon^s)$ is the neighboring nodes connected to node v_ϵ^s . Meanwhile, let $\mathcal{G}_{\text{k, ita}} = \{\mathcal{V}, \mathcal{E}_{\text{k, ita}}\}$ be the k -hop intra-scale hypergraph, where $\mathcal{E}_{\text{k, ita}} = \{\mathcal{E}_{\text{k, ita}}^s \mid s \in \{1, \dots, S\}\}$ contains

k -hop intra-scale hyperedge sets of different scales. The i th hyperedge of scale s based on k -hop connections $e_{i,k}^s \in \mathcal{E}_{k,\text{ita}}^s$ is defined as follows:

$$e_{i,k}^s = \{v_d^s, v_{d+k}^s, \dots, v_{d+(H_s-1)k}^s\}, \quad (6)$$

where d is the starting node index under the i th hyperedge of scale s based on k -hop connections, which can be defined as follows:

$$d = \left\lfloor \frac{i-1}{k} \right\rfloor \times H_s k + (i-1) \% k + 1, \quad (7)$$

where k is the temporal distance between two neighboring nodes. The intra-scale hypergraph $\mathcal{G}_{\text{ita}} = \{\mathcal{V}, \mathcal{E}_{\text{ita}}\}$ based on the original intra-scale hypergraph and the k -hop intra-scale hypergraph can be formulated as follows:

$$\mathcal{G}_{\text{ita}} = \text{concat}(\mathcal{G}_{\text{o,ita}}, \mathcal{G}_{k,\text{ita}}), \quad (8)$$

where *concat* denotes the concatenation operation. High-order interactions between temporal patterns not only exist between intra-scale temporal patterns, but also between inter-scale temporal patterns, e.g., interactions between hourly and daily patterns, and interactions between daily and weekly patterns. In addition, there are temporal pattern interactions across all scales, e.g., interactions between hourly, daily, and weekly patterns. Therefore, we design the inter-scale hypergraph and mixed-scale hypergraph.

Inter-Scale Hypergraph. As shown in Figure 2(b), the inter-scale hypergraph $\mathcal{G}_{\text{ite}} = \{\mathcal{V}, \mathcal{E}_{\text{ite}}\}$ is obtained by concatenating the original inter-scale hypergraph and k -hop inter-scale hypergraph. Mathematically, let $\mathcal{G}_{\text{o,ite}} = \{\mathcal{V}, \mathcal{E}_{\text{o,ite}}\}$ be the original inter-scale hypergraph, where $\mathcal{E}_{\text{o,ite}} = \{\mathcal{E}_{\text{o,ite}}^s\}_{s \in \{1, \dots, S\}}$ contains original inter-scale hyperedge sets of different scales. The i th hyperedge of scale s $e_i^s \in \mathcal{E}_{\text{o,ite}}^s$ is defined as follows:

$$e_i^s = \left\{ v_{\lceil \frac{i}{l^s} \rceil}^{s+1}, v_{\lceil \frac{i}{l^s} \rceil}^s, v_{\lceil \frac{i}{l^s} \rceil + 1}^s, \dots, v_{\lceil \frac{i}{l^s} \rceil + H_s}^s \right\}, \quad (9)$$

where l^s denotes the size of the aggregation window at scale s . Then, let $\mathcal{G}_{k,\text{ite}} = \{\mathcal{V}, \mathcal{E}_{k,\text{ite}}\}$ be the k -hop inter-scale hypergraph, where $\mathcal{E}_{k,\text{ite}} = \{\mathcal{E}_{k,\text{ite}}^s\}_{s \in \{1, \dots, S\}}$ contains k -hop inter-scale hyperedge sets of different scales and $e_{i,k}^s \in \mathcal{E}_{k,\text{ite}}^s$ is defined as follows:

$$e_{i,k}^s = \{v_{\lceil \frac{i}{l^s} \rceil}^{s+1}, v_{\lceil \frac{i}{l^s} \rceil}^s, v_{\lceil \frac{i}{l^s} \rceil + k}^s, \dots, v_{\lceil \frac{i}{l^s} \rceil + (H_s-1)k}^s\}. \quad (10)$$

Mixed-Scale Hypergraph. As shown in Figure 2(c), the mixed-scale hypergraph $\mathcal{G}_{\text{mix}} = \{\mathcal{V}, \mathcal{E}_{\text{mix}}\}$ is obtained by concatenating the original mixed-scale hypergraph and k -hop mixed-scale hypergraph. Mathematically, let $\mathcal{G}_{\text{o,mix}} = \{\mathcal{V}, \mathcal{E}_{\text{o,mix}}\}$ be the original mixed-scale hypergraph, where $\mathcal{E}_{\text{o,mix}}$ denotes the original mixed-scale hyperedge set. The i th hyperedge $e_i \in \mathcal{E}_{\text{o,mix}}$ is defined as follows:

$$e_i = \left\{ v_{\delta_s}^s, v_{\delta_{s-1}}^{s-1}, \dots, v_{\delta_1}^1, v_{\delta_1+1}^1, \dots, v_{\delta_1+H-1}^1 \right\}, \quad (11)$$

where $\delta_s = \lceil \epsilon / (1 \times \prod_{\alpha=2}^s l^\alpha) \rceil$ is the starting node index of scale s under the i th hyperedge based on original connections. Then, let $\mathcal{G}_{k,\text{mix}} = \{\mathcal{V}, \mathcal{E}_{k,\text{mix}}\}$ be the k -hop mixed-scale hypergraph, where $\mathcal{E}_{k,\text{mix}}$ denotes the k -hop mixed-scale hyperedge set. $e_{i,k} \in \mathcal{E}_{k,\text{mix}}$ is defined as follows:

$$e_{i,k} = \left\{ v_{\delta_{s,k}}^s, v_{\delta_{s-1,k}}^{s-1}, \dots, v_{\delta_1}^1, v_{\delta_1+k}^1, \dots, v_{\delta_1+(H-1)k}^1 \right\}, \quad (12)$$

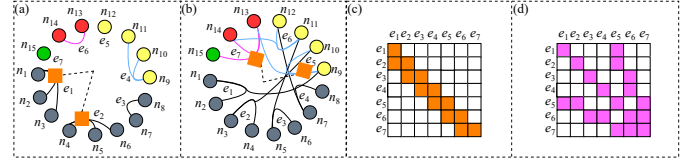


Figure 3: Hyperedge graph construction. (a) and (b) are the sequential relationship and association relationship, respectively. (c) and (d) are the constructed adjacency matrix based on the sequential relationship and association relationship, respectively.

where $\delta_{s,k} = \lceil d / (1 \times \prod_{\alpha=2}^s l^\alpha) \rceil$ is the starting node index of scale s under the i th hyperedge based on k -hop connections.

The final hypergraph $\mathcal{G} = \{\mathcal{V}, \mathcal{E}\}$ is obtained by considering the abovementioned three hypergraphs, which can be formulated as follows:

$$\mathcal{G} = \text{concat}(\mathcal{G}_{\text{ita}}, \mathcal{G}_{\text{ite}}, \mathcal{G}_{\text{mix}}). \quad (13)$$

Hyperedge Graph Construction

After building the hypergraph, to enhance hypergraph modeling, we build the hyperedge graph to model interactions between hyperedges. Specifically, we build the hyperedge graph by representing hyperedges in \mathcal{G} as nodes and considering the sequential relationship and association relationship. Let $G = (V, E, \mathbf{A})$ be the hyperedge graph, where $V = \{v_{e_i} | v_{e_i} \in \mathcal{E}\}$ is the node set of G and $E = \{(v_{e_i}, v_{e_j}) | v_{e_i}, v_{e_j} \in \mathcal{E}\}$ is the edge set of G . \mathbf{A} is the weighted adjacency matrix defined based on the sequential relationship and association relationship between hyperedges.

Sequential Relationship. Within the intra-scale hypergraph, two hyperedges that connect nodes with temporal order exhibit the sequential relationship. For example, as shown in Figure 3(a), hyperedge e_1 connects the previous three nodes, and hyperedge e_2 connects the next three nodes. Since long-range time series is a collection of data points arranged in chronological order, intuitively, changes (e.g., increase, decrease, or fluctuation) in the values of nodes connected by e_1 may influence the values of nodes connected by e_2 . Formally, let $G_{\text{sr}} = (V_{\text{sr}}, E_{\text{sr}}, \mathbf{A}_{\text{sr}})$ represent the hyperedge graph constructed based on the sequential relationship, where $V_{\text{sr}} = \{v_{e_{sr}} | v_{e_{sr}} \in \mathcal{E}_{\text{ita}}\} \in \mathbb{R}^{D_{\text{sr}} \times D}$ is the node set and D_{sr} is the number of intra-scale hyperedges. $E_{\text{sr}} = \{(v_{e_{i,\text{sr}}}, v_{e_{j,\text{sr}}}) | v_{e_{i,\text{sr}}}, v_{e_{j,\text{sr}}} \in \mathcal{E}_{\text{ita}}, 0 \leq i - j \leq 1\}$ denotes the edge set constructed based on the sequential relationship. As shown in Figure 3(c), the adjacency matrix constructed based on the sequential relationship $\mathbf{A}_{\text{sr}} \in \mathbb{R}^{D_{\text{sr}} \times D_{\text{sr}}}$ is defined as follows:

$$\mathbf{A}_{\text{sr}} = \{\mathbf{A}_{ij,\text{sr}} | \mathbf{A}_{ij,\text{sr}} = 1 \text{ if } (v_{e_{i,\text{sr}}}, v_{e_{j,\text{sr}}}) \in E_{\text{sr}}, \text{ else } 0\}. \quad (14)$$

Association Relationship. Within the inter-scale hypergraph and mixed-scale hypergraph, we define hyperedges with common nodes have an association relationship. As shown in Figure 3(b), e_5 and e_7 have an association relationship, as they share a common node n_{13} . Formally, let $G_{\text{ar}} = (V_{\text{ar}}, E_{\text{ar}}, \mathbf{A}_{\text{ar}})$ represent the hyperedge graph constructed based on the association relationship, where $V_{\text{ar}} = \{v_{e_{ar}} | v_{e_{ar}} \in \{\mathcal{E}_{\text{ite}}, \mathcal{E}_{\text{mix}}\}\} \in \mathbb{R}^{D_{\text{ar}} \times D}$ is the node set of G_{ar} and D_{ar} is the number sum of inter-scale hyperedges and

mixed-scale hyperedges. $E_{\text{ar}} = \{(v_{e_i, \text{ar}}, v_{e_j, \text{ar}}) | v_{e_i, \text{ar}}, v_{e_j, \text{ar}} \in \{\mathcal{E}_{\text{ite}}, \mathcal{E}_{\text{mix}}\}, |v_{e_i, \text{ar}} \cap v_{e_j, \text{ar}}| \geq 1\}$ denotes the edge set of G_{ar} . As shown in Figure 3(d), the adjacency matrix based on the association relationship $\mathbf{A}_{\text{ar}} \in \mathbb{R}^{D_{\text{ar}} \times D_{\text{ar}}}$ is defined as follows:

$$\mathbf{A}_{\text{ar}} = \{\mathbf{A}_{ij, \text{ar}} | \mathbf{A}_{ij, \text{ar}} = 1 \text{ if } (v_{e_i, \text{ar}}, v_{e_j, \text{ar}}) \in E_{\text{ar}}, \text{ else } 0\}. \quad (15)$$

The adjacency matrix \mathbf{A} based on the above two relationships can be defined as follows:

$$\mathbf{A} = \begin{bmatrix} \mathbf{A}_{\text{sr}} & \mathbf{\Gamma}_1 \\ \mathbf{\Gamma}_2 & \mathbf{A}_{\text{ar}} \end{bmatrix} \in \mathbb{R}^{D_{\varphi} \times D_{\varphi}}, \quad (16)$$

where $\mathbf{\Gamma}_1 \in \mathbb{R}^{D_{\text{sr}} \times D_{\text{ar}}}$ and $\mathbf{\Gamma}_2 \in \mathbb{R}^{D_{\text{ar}} \times D_{\text{sr}}}$ are matrices consisting entirely of zeros, and D_{φ} is the sum of D_{ar} and D_{sr} .

4.3 Tri-Stage Message Passing Mechanism

After building the hypergraph and hyperedge graph, to aggregate pattern information and learn the interaction strength between temporal patterns of different scales, we propose a TMP mechanism, which contains the node-hyperedge, hyperedge-hyperedge, and hyperedge-node phases.

Node-Hyperedge Phase. Given the sequences based on the MFE module $\mathbf{X} = \{\mathbf{X}^1, \mathbf{X}^2, \dots, \mathbf{X}^S\} \in \mathbb{R}^{N \times D}$, where N denotes the number sum of input time steps and aggregated feature values of different scales. We first get the initialized node embeddings $\mathbf{V} = f(\mathbf{X}) \in \mathbb{R}^{N \times D}$, where f can be implemented by the multi-layer perceptron (MLP). As shown in Figure 1(c), we get the initialized hyperedge embeddings by the aggregation operation based on the hypergraph \mathcal{G} . Specifically, for the i th hyperedge $e_i \in \mathcal{E}$, its initialized embedding is obtained as follows:

$$\mathbf{v}_{e_i} = \sum_{v_j \in \mathcal{N}(e_i)} \mathbf{v}_j \in \mathbb{R}^D, \quad (17)$$

where $\mathcal{N}(e_i)$ denotes neighboring nodes connected by e_i .

Hyperedge-Hyperedge Phase. After getting initialized hyperedge embeddings, we proceed to update their embeddings through the constructed hyperedge graph. Specifically, for the given initialized hyperedge embeddings $\mathbf{V} = \{\mathbf{v}_{e_i} | \mathbf{v}_{e_i} \in \mathcal{E}\} \in \mathbb{R}^{M \times D}$, we transform it into query $\tilde{\mathbf{Q}} = \mathbf{V}\mathbf{W}^q$, key $\tilde{\mathbf{K}} = \mathbf{V}\mathbf{W}^k$, and value $\tilde{\mathbf{V}} = \mathbf{V}\mathbf{W}^v$, where \mathbf{W}^q , \mathbf{W}^k , and \mathbf{W}^v are learnable weight matrices. For the i th row $\tilde{\mathbf{q}}_i \in \tilde{\mathbf{Q}}$, the updated hyperedge embedding $\tilde{\mathbf{v}}_{e_i} \in \tilde{\mathbf{V}}_e$ can be calculated as follows:

$$\tilde{\mathbf{v}}_{e_i} = \sum_{j=1}^M \frac{\exp(e_{ij})}{\sum_{\ell=1}^M \exp(e_{i\ell})} \tilde{\mathbf{v}}_j \quad (18)$$

$$e_{ij} = \frac{\tilde{\mathbf{q}}_i \tilde{\mathbf{k}}_j^T}{\sqrt{D}} - (1 - \mathbf{A}_{ij})\mathbf{C},$$

where $\tilde{\mathbf{k}}_j^T$ denotes the transpose of the j th row in $\tilde{\mathbf{K}}$ and $\tilde{\mathbf{v}}_j$ denotes the j th row in $\tilde{\mathbf{V}}$. $\mathbf{A}_{ij} \in \mathbf{A}$ is a binary value and \mathbf{C} is a large constant.

Hyperedge-Node Phase. After obtaining the updated hyperedge embeddings, we update the node embeddings by considering all the related hyperedges. Considering the constructed hypergraph \mathcal{G} , we use the hypergraph convolution

to update the node embeddings. Specifically, the symmetric normalized hypergraph Laplacian convolution can be formulated as follows:

$$\tilde{\mathbf{V}} = \sigma(\mathbf{D}_v^{-1/2} \mathbf{H} \mathbf{D}_e^{-1} \mathbf{H}^T \mathbf{D}_v^{-1/2} \mathbf{V} \mathbf{P}) \in \mathbb{R}^{N \times D_e}, \quad (19)$$

where $\tilde{\mathbf{V}}$ is the output of the hypergraph convolution and D_e is the output dimension. $\mathbf{P} \in \mathbb{R}^{D_e \times D_e}$ denotes the learnable parameters and σ is the activation function, e.g., LeakyReLU and ELU. To capture the interaction strength of each node $v_i \in \mathcal{V}$ and its related hyperedges, we dynamically update \mathbf{H} using the node embedding and updated hyperedge embeddings, which can be formulated as follows:

$$\mathbf{H}_{ij}^{\text{att}} = \frac{\exp(\sigma(f_t[\mathbf{v}_i, \tilde{\mathbf{v}}_{e_j}]))}{\sum_{k \in \mathcal{N}_i} \exp(\sigma(f_t[\mathbf{v}_i, \tilde{\mathbf{v}}_{e_k}]))}, \quad (20)$$

where $[\cdot, \cdot]$ denotes the concatenation operation of the node and its related hyperedges. f_t is a trainable MLP, and \mathcal{N}_i is the neighboring hyperedges connected to v_i , which can be accessed using the constructed hypergraph \mathcal{G} . Then, we use Equation 19 to aggregate pattern information of different scales by replacing \mathbf{H} with \mathbf{H}^{att} . The multi-head attention mechanism is also used to stabilize the training process:

$$\tilde{\mathbf{V}} = \bigoplus_{j=1}^{\mathcal{J}} (\sigma(\mathbf{D}_v^{-1/2} \mathbf{H}_j^{\text{att}} \mathbf{D}_e^{-1} \mathbf{H}_j^{\text{att}T} \mathbf{D}_v^{-1/2} \mathbf{V} \mathbf{P}_j)), \quad (21)$$

where \bigoplus is the aggregation function used for combing the outputs of multi-head, e.g., concatenation or average pooling. $\mathbf{H}_j^{\text{att}}$ and \mathbf{P}_j are the enriched incidence matrix and the learnable weight matrix of the j th head, respectively. \mathcal{J} is the number of heads.

4.4 Objective Function

After obtaining the updated node embeddings encoded by the multi-scale hypergraph, we concatenate the last node embeddings of each sub-sequence from different scales and then put them into a linear layer for prediction. We choose MSE as our objective function, which is defined as follows:

$$\mathcal{L} = \frac{1}{H} \left\| \hat{\mathbf{X}}_{T+1:T+H}^{\text{O}} - \mathbf{X}_{T+1:T+H}^{\text{O}} \right\|_2^2, \quad (22)$$

where $\hat{\mathbf{X}}_{T+1:T+H}^{\text{O}}$ and $\mathbf{X}_{T+1:T+H}^{\text{O}}$ are ground truth and forecasting results, respectively.

5 Experiments

5.1 Experimental Setup

Datasets. We conduct experiments on five commonly used long-range time series forecasting datasets, including *ETT* (*ETTh* and *ETTm*), *Electricity*, *Weather*, and *Traffic* datasets. The descriptions about the five datasets are as follows:

ETT [Zhou *et al.*, 2021]: This dataset contains the oil temperature and load data collected by electricity transformers, including *ETTh* (*ETTh1* and *ETTh2*) and *ETTm* (*ETTm1* and *ETTm2*), which are sampled hourly and every 15 minutes, respectively.

Table 1: Multivariate long-range time series forecasting results on five real-world datasets. The input length is set as $I = 168$, and the prediction length O is set as 96, 168, 336, and 720 (For *ETTm1*, the prediction length is set as 96, 288, 672, and 720). IMP shows the improvement of MSHyper over the best baseline. The best results are **bolded** and the second best results are underlined.

Methods		Informer (AAAI 2021)		Autoformer (NeurIPS 2021)		Pyraformer (ICLR 2021)		FEDformer (ICML 2022)		Quatformer (KDD 2022)		Crossformer (ICLR 2023)		MSHyper (Ours)		IMP	
Metric		MSE	MAE	MSE	MAE	MSE	MAE	MSE	MAE	MSE	MAE	MSE	MAE	MSE	MAE	MSE	MAE
Weather	96	0.300	0.384	0.266	0.336	0.503*	0.518*	0.217	0.296	<u>0.211</u>	<u>0.279</u>	0.444*	0.473*	0.164	0.217	22.27%	22.22%
	168	0.608	0.567	0.574	0.548	0.519	0.521	0.564	0.541	<u>0.251*</u>	<u>0.295*</u>	0.473	0.494	0.197	0.246	21.51%	16.61%
	336	0.702	0.620	0.600	0.571	0.539	0.543	0.533	0.536	<u>0.310</u>	<u>0.344</u>	0.495	0.515	0.262	0.298	15.48%	13.37%
	720	0.831	0.731	0.587	0.570	0.547	0.553	0.562	0.557	<u>0.381</u>	<u>0.374</u>	0.526	0.542	0.309	0.325	18.90%	13.10%
Electricity	96	0.274	0.368	0.255	0.339	0.272*	0.371*	0.183	0.297	0.197	0.308	<u>0.185*</u>	<u>0.278*</u>	0.183	0.271	0%	2.52%
	168	0.368	0.424	0.299	0.387	0.452	0.455	0.263	0.361	<u>0.205*</u>	0.315*	0.231	<u>0.309</u>	0.193	0.298	5.85%	3.56%
	336	0.381	0.431	0.375	0.428	0.463	0.456	0.305	0.386	<u>0.220</u>	<u>0.329</u>	0.323	0.369	0.205	0.310	6.82%	5.78%
	720	0.406	0.443	0.377	0.434	0.480	0.461	0.372	0.434	<u>0.245</u>	<u>0.350</u>	0.404	0.423	0.230	0.329	6.12%	6.00%
ETTh1	96	0.865	0.713	0.449	0.459	0.701*	0.635*	<u>0.376</u>	0.419	0.422*	0.447*	0.396*	<u>0.412*</u>	0.375	0.398	0.27%	3.40%
	168	0.931	0.752	0.493	0.479	0.781	0.675	0.412	0.449	0.453	0.489	<u>0.410</u>	<u>0.441</u>	0.405	0.427	1.22%	3.17%
	336	1.128	0.873	0.509	0.492	0.912	0.747	0.456	0.474	0.491	0.495	<u>0.440</u>	<u>0.461</u>	0.428	0.439	2.73%	4.77%
	720	1.215	0.896	0.539	0.537	0.993	0.792	0.521	0.515	0.523	0.525	0.519	0.524	0.503	0.507	3.08%	1.55%
ETTm1	96	0.678	0.614	0.502	0.476	0.520	0.504	0.366	0.412	0.375	0.398	<u>0.320</u>	<u>0.373</u>	0.315	0.365	1.56%	2.14%
	288	1.056	0.786	0.604	0.522	0.729	0.657	<u>0.398</u>	0.433	0.408	<u>0.424</u>	0.404	0.427	0.394	0.419	1.01%	1.17%
	672	1.192	0.926	0.607	0.530	0.980	0.678	<u>0.455</u>	<u>0.464</u>	0.472*	0.468*	0.569	0.528	0.451	0.462	0.88%	0.43%
	720	1.166	0.823	0.671	0.561	0.912*	0.727*	0.543	0.490	0.499	0.502	0.751*	0.677*	0.493	0.471	1.20%	3.88%
Traffic	96	0.719	0.391	0.613	0.388	0.628*	0.354*	0.587	0.366	0.618	0.384	<u>0.450*</u>	0.477*	0.408	0.269	9.33%	24.01%
	168	0.660	0.391	0.649	0.407	0.635	0.347	0.607	0.385	0.621*	0.399*	<u>0.513</u>	<u>0.289</u>	0.418	0.271	18.52%	6.23%
	336	0.747	0.405	0.624	0.388	0.641	0.347	0.624	0.389	0.622	0.384	<u>0.530</u>	<u>0.300</u>	0.431	0.287	18.68%	4.33%
	720	0.792	0.430	0.674	0.417	0.670	0.364	0.623	0.378	0.629	0.383	<u>0.573</u>	<u>0.313</u>	0.463	0.298	19.20%	4.79%

* indicates that some methods do not have uniform prediction lengths with other methods. To ensure a fair comparison, we utilize their official code and adjust prediction lengths.

*Electricity*¹: This dataset contains the electricity consumption of 321 clients from the UCI Machine Learning Repository, which is sampled hourly.

*Traffic*²: This dataset contains the road occupancy rates of 862 sensors in San Francisco Bay Area freeways, which is sampled hourly.

*Weather*³: This dataset contains 21 meteorological measurements data from the Weather Station of the Max Planck Biogeochemistry, which is sampled every 10 minutes.

Following existing works [Zhou *et al.*, 2021; Zhang and Yan, 2023; Liu *et al.*, 2021], we split each dataset into training, validation, and testing set based on chronological order. The ratio is 6:2:2 for the *ETT* dataset and 7:2:1 for the others.

Experimental Settings. MSHyper is trained/tested on a single NVIDIA Geforce RTX 3090 GPU. The aggregation windows are set to 4 for *ETTh* and *ETTm* datasets and 3 for other datasets. S and H in MSHyper are set to 4 in all experiments. Z-Score normalization is used to normalize all datasets. MSE and MAE are used as evaluation metrics. Lower MSE and MAE results mean better performance. Adam is set as the optimizer with the initial learning rate of 10^{-4} , and the batch size is set to 32.

Baselines. The baselines include six latest Transformer-based models: Informer [Zhou *et al.*, 2021], Autoformer [Wu *et al.*, 2021], Pyraformer [Liu *et al.*, 2021], FEDformer [Zhou *et al.*, 2022], Quatformer [Chen *et al.*, 2022], and Crossformer [Zhang and Yan, 2023]. The source code of MSHyper is released on Anonymous GitHub⁴.

5.2 Main Results

Multivariate Results. Table 1 shows the multivariate experimental results of MSHyper compared with baselines on five

datasets. We can see that MSHyper achieves state-of-the-art (SOTA) results on all five datasets at all prediction lengths. From Table 1 we can discern the following tendencies: 1) Informer and Autoformer exhibit relatively poor predictive performance. This may come from that time series forecasting requires modeling temporal pattern interactions, while vanilla attention or simplistic decomposition techniques are insufficient in capturing such interactions. 2) By considering the temporal pattern interactions of different scales, Pyraformer, Crossformer, FEDformer, and Quatformer all achieve excellent performance. 3) Benefiting from its ability to model high-order temporal pattern interactions, MSHyper achieves the best performance in long-range time series forecasting. Specifically, MSHyper reduces prediction errors by an average of 8.73% and 7.15% over the best baseline in MSE and MAE, respectively.

Univariate Results. Table 2 summarizes the results of univariate long-range time series forecasting on *ETTh* (*ETTh1* and *ETTh2*) and *ETTm* (*ETTm1* and *ETTm2*) datasets. We can see from Table 2 that MSHyper achieves SOTA results on all datasets at all prediction lengths. Specifically, MSHyper gives an average error reduction of 9.57% and 7.09% compared to the best baseline in MSE and MAE, respectively. The experimental results verify the effectiveness of MSHyper in univariate long-range time series forecasting.

5.3 Ablation Studies

We conduct ablation studies to verify the impact of different components on long-range time series forecasting. All ablation studies are conducted on *ETTh1* dataset.

Multi-Scale Hypergraph. To investigate the effectiveness of the multi-scale hypergraph, we conduct ablation studies by carefully designing the following three variants: 1) Replacing the H-HGC model with the fully-connected graph (MSHyper-FCG). 2) Replacing the H-HGC model with the pyramid graph used in [Liu *et al.*, 2021] (MSHyper-PG). 3) Connecting the input sequence with intra-scale hyperedges, and thus the multi-scale hypergraph turns to the single-scale

¹<https://archive.ics.uci.edu/ml/datasets/ElectricityLoadDiagrams20112014>

²<http://pems.dot.ca.gov>

³<https://www.bgc-jena.mpg.de/wetter/>

⁴<https://anonymous.4open.science/r/MSHyper-A3FF>

Table 2: Univariate long-range time series forecasting results on *ETT* dataset. The input length is set as $I=168$, and the prediction length O is set as 96, 192, 336, and 720. IMP shows the improvement of MSHyper over the best baseline. The best results are **bolded** and the second best results are underlined.

Methods		Informer (AAAI 2021)		Autoformer (NeurIPS2021)		Pyraformer* (ICLR 2021)		FEDformer (ICML 2022)		Quatformer* (KDD 2022)		Crossformer* (ICLR 2023)		MSHyper (Ours)		IMP	
Metric		MSE	MAE	MSE	MAE	MSE	MAE	MSE	MAE	MSE	MAE	MSE	MAE	MSE	MAE	MSE	MAE
ETTh1	96	0.193	0.377	0.071	<u>0.206</u>	0.099	0.277	0.079	0.215	<u>0.069</u>	0.222	0.076	0.216	0.060	0.187	13.04%	9.22%
	192	0.217	0.395	0.114	0.262	0.174	0.346	0.104	0.245	0.138	<u>0.222</u>	<u>0.085</u>	0.225	0.078	0.215	8.24%	3.15%
	336	0.202	0.381	0.107	0.258	0.198	0.370	0.119	0.270	0.123	0.275	<u>0.106</u>	<u>0.257</u>	0.087	0.226	17.92%	12.06%
	720	0.183	0.355	<u>0.126</u>	<u>0.283</u>	0.209	0.384	0.142	0.299	0.146	0.293	0.128	0.287	0.108	0.230	14.29%	18.73%
ETTh2	96	0.213	0.373	0.153	0.306	0.152	0.303	0.128	<u>0.271</u>	0.135	0.278	<u>0.125</u>	0.273	0.117	0.266	6.40%	1.85%
	192	0.227	0.387	0.204	0.351	0.197	0.348	<u>0.185</u>	<u>0.330</u>	0.189	0.342	0.187	0.334	0.172	0.325	7.03%	1.52%
	336	0.242	0.401	0.246	0.389	0.238	0.385	0.231	0.378	0.234	<u>0.375</u>	<u>0.227</u>	0.377	0.222	0.373	2.20%	0.53%
	720	0.291	0.439	0.268	<u>0.409</u>	0.274	0.435	0.278	0.420	<u>0.263</u>	0.424	0.266	0.410	0.242	0.401	7.98%	1.96%
ETTm1	96	0.109	0.277	0.056	0.183	0.127	0.281	<u>0.033</u>	<u>0.140</u>	0.035	0.147	0.035	0.145	0.032	0.136	3.03%	2.86%
	192	0.151	0.310	0.081	0.216	0.205	0.343	0.058	0.186	0.174	0.193	<u>0.055</u>	<u>0.180</u>	0.049	0.168	10.91%	6.67%
	336	0.427	0.591	0.076	0.218	0.302	0.457	0.084	0.231	0.105	0.237	<u>0.072</u>	<u>0.209</u>	0.066	0.195	8.33%	6.70%
	720	0.438	0.586	0.110	0.267	0.387	0.485	0.102	0.250	0.112	0.264	<u>0.097</u>	<u>0.248</u>	0.087	0.224	10.31%	9.68%
ETTm2	96	0.088	0.225	0.065	0.189	0.074	0.208	0.067	0.198	0.075	0.217	<u>0.058</u>	<u>0.183</u>	0.047	0.165	18.97%	9.84%
	192	0.132	0.283	0.118	0.256	0.116	0.252	<u>0.102</u>	0.245	0.117	0.263	0.105	<u>0.237</u>	0.094	0.212	7.84%	10.55%
	336	0.180	0.336	0.154	0.305	0.143	0.295	<u>0.130</u>	<u>0.279</u>	0.145	0.286	0.133	0.280	0.123	0.242	5.38%	13.26%
	720	0.300	0.435	0.182	0.335	0.197	0.338	<u>0.178</u>	<u>0.325</u>	0.183	0.368	0.181	<u>0.324</u>	0.158	0.308	11.24%	4.94%

* indicates that some methods do not yield results for univariate long-range time series forecasting. To ensure a fair comparison, we utilize their official code and fine-tune key hyperparameters via grid search. Other results are from FEDformer.

hypergraph (MSHyper-SSH). The experimental results are shown in Table 3, from which we can observe that MSHyper performs the best in all cases, which indicates the importance of multi-scale hypergraph in modeling high-order interactions between temporal patterns of different scales.

Table 3: Results of different multi-scale hypergraph construction methods.

Methods		Prediction length		
		168	336	720
MSHyper-FCG	MSE	1.035	1.079	1.247
	MAE	0.863	0.785	0.896
MSHyper-PG	MSE	0.712	0.882	0.892
	MAE	0.649	0.725	0.747
MSHyper-SSH	MSE	0.601	0.643	0.674
	MAE	0.568	0.587	0.629
MSHyper	MSE	0.405	0.428	0.503
	MAE	0.427	0.439	0.507

Hyperedge Graph. To investigate the effectiveness of the hyperedge graph, we conduct ablation studies by carefully designing the following three variants: 1) Removing the association relationship of the hyperedge graph (MSHyper-w/o AR). 2) Removing the sequential relationship of the hyperedge graph (MSHyper-w/o SR). 3) Removing the hyperedge graph, i.e., without the hyperedge-hyperedge phase (MSHyper-w/o H-H). The experimental results are shown in Table 4. We can observe that MSHyper performs better than MSHyper-w/o AR and MSHyper-w/o SR, showing the effectiveness of the association relationship and sequential relationship, respectively. In addition, removing the hyperedge-hyperedge phase gets the worst forecasting results, which demonstrates the superiority of the hyperedge graph in enhancing hypergraph modeling.

5.4 Parameter Studies

We also perform parameter studies to measure the impact of the aggregation function, k -hop, and input length on *ETTh1* dataset. The experimental results are shown in Table 5, Figure 4, and Figure 5, from which we can observe that: 1) The results based on the convolution operation outperform those based on other operations, possibly because convolution ker-

Table 4: Results of different hyperedge graph construction methods.

Methods		Prediction length		
		168	336	720
MSHyper-w/o AR	MSE	0.413	0.438	0.514
	MAE	0.429	0.445	0.505
MSHyper-w/o SR	MSE	0.408	0.433	0.507
	MAE	0.419	0.452	0.516
MSHyper-w/o H-H	MSE	0.430	0.531	0.612
	MAE	0.474	0.506	0.598
MSHyper	MSE	0.405	0.428	0.503
	MAE	0.427	0.439	0.507

Table 5: Impact of aggregation function.

Methods		Prediction length		
		168	336	720
Max-pooling	MSE	0.508	0.437	0.513
	MAE	0.468	0.457	0.524
Average-pooling	MSE	0.532	0.431	0.512
	MAE	0.506	0.455	0.523
Conv	MSE	0.405	0.428	0.503
	MAE	0.427	0.439	0.507

nels can extract more complex features. 2) The best performance can be obtained when the k -hop is 4. The reason may be that a small k -hop limits interactions to the neighboring nodes, and a large k -hop would introduce noises. 3) MSHyper achieves the optimal performance when the input length is 168. The reason may be that the sequence with a shorter input length contains insufficient pattern information, while the sequence with a longer input length introduces more noise interference for high-order pattern interactions.

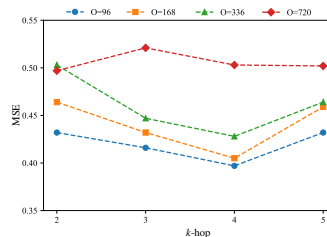


Figure 4: Impact of k -hop.

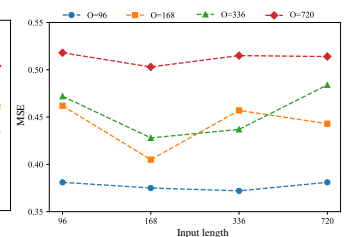


Figure 5: Impact of input length.

6 Conclusions

In this paper, we propose MSHyper for long-range time series forecasting. Specifically, the H-HGC module is introduced

to provide foundations for modeling high-order interactions between temporal patterns. The TMP mechanism is employed to aggregate high-order pattern information and learn the interaction strength between temporal patterns of different scales. Extensive experiments on five real-world datasets show the superiority of MSHyper.

References

- [Ainslie *et al.*, 2020] Joshua Ainslie, Santiago Ontanon, Chris Alberti, Vaclav Cvicek, Zachary Fisher, Philip Pham, Anirudh Ravula, Sumit Sanghai, Qifan Wang, and Li Yang. ETC: Encoding long and structured inputs in transformers. In *Proceedings of the International Conference on Empirical Methods in Natural Language Processing*, pages 268–284, 2020.
- [Bai *et al.*, 2018] Shaojie Bai, J Zico Kolter, and Vladlen Koltun. An empirical evaluation of generic convolutional and recurrent networks for sequence modeling. *arXiv preprint arXiv:1803.01271*, 2018.
- [Bai *et al.*, 2021] Song Bai, Feihu Zhang, and Philip HS Torr. Hypergraph convolution and hypergraph attention. *Pattern Recognition*, 110(1):1–8, 2021.
- [Box and Jenkins, 1968] George EP Box and Gwilym M Jenkins. Some recent advances in forecasting and control. *Journal of the Royal Statistical Society Series C*, 17(2):91–109, 1968.
- [Chen *et al.*, 2021] Zipeng Chen, Qianli Ma, and Zhenxi Lin. Time-aware multi-scale RNNs for time series modeling. In *Proceedings of the International Joint Conference on Artificial Intelligence*, pages 2285–2291, 2021.
- [Chen *et al.*, 2022] Weiqi Chen, Wenwei Wang, Bingqing Peng, Qingsong Wen, Tian Zhou, and Liang Sun. Learning to rotate: Quaternion transformer for complicated periodic time series forecasting. In *Proceedings of the ACM SIGKDD Conference on Knowledge Discovery and Data Mining*, pages 146–156, 2022.
- [Chen *et al.*, 2023a] Ling Chen, Donghui Chen, Zongjiang Shang, Binqing Wu, Cen Zheng, Bo Wen, and Wei Zhang. Multi-scale adaptive graph neural network for multivariate time series forecasting. *IEEE Transactions on Knowledge and Data Engineering*, 35(10):10748–10761, 2023.
- [Chen *et al.*, 2023b] Zonglei Chen, Minbo Ma, Tianrui Li, Hongjun Wang, and Chongshou Li. Long sequence time-series forecasting with deep learning: A survey. *Information Fusion*, 97(1):1–36, 2023.
- [Cirstea *et al.*, 2022] Razvan-Gabriel Cirstea, Chenjuan Guo, Bin Yang, Tung Kieu, Xuanyi Dong, and Shirui Pan. Triformer: Triangular, variable-specific attentions for long sequence multivariate time series forecasting. In *Proceedings of the International Joint Conference on Artificial Intelligence*, pages 1–10, 2022.
- [Dosovitskiy *et al.*, 2021] Alexey Dosovitskiy, Lucas Beyer, Alexander Kolesnikov, Dirk Weissenborn, Xiaohua Zhai, Thomas Unterthiner, Mostafa Dehghani, Matthias Minderer, Georg Heigold, Sylvain Gelly, Jakob Uszkoreit, and Neil Houlsby. An image is worth 16x16 words: Transformers for image recognition at scale. In *Proceedings of the International Conference on Learning Representations*, 2021.
- [Feng *et al.*, 2019] Yifan Feng, Haoxuan You, Zizhao Zhang, Rongrong Ji, and Yue Gao. Hypergraph neural networks. In *Proceedings of the AAAI Conference on Artificial Intelligence*, pages 3558–3565, 2019.
- [Guo *et al.*, 2019] Qipeng Guo, Xipeng Qiu, Pengfei Liu, Yunfan Shao, Xiangyang Xue, and Zheng Zhang. Star-transformer. In *Proceedings of the International Conference of the North American Chapter of the Association for Computational Linguistics: Human Language Technologies*, pages 1315–1325, 2019.
- [Kitaev *et al.*, 2020] Nikita Kitaev, Łukasz Kaiser, and Anselm Levskaya. Reformer: The efficient transformer. In *Proceedings of the International Conference on Learning Representations*, 2020.
- [Lai *et al.*, 2018] Guokun Lai, Wei-Cheng Chang, Yiming Yang, and Hanxiao Liu. Modeling long-and short-term temporal patterns with deep neural networks. In *Proceedings of the International ACM SIGIR Conference on Research and Development in Information Retrieval*, pages 95–104, 2018.
- [Li *et al.*, 2019] Shiyang Li, Xiaoyong Jin, Yao Xuan, Xiyou Zhou, Wenhui Chen, Yu-Xiang Wang, and Xifeng Yan. Enhancing the locality and breaking the memory bottleneck of transformer on time series forecasting. *Advances in Neural Information Processing Systems*, pages 1–11, 2019.
- [Liu *et al.*, 2021] Shizhan Liu, Hang Yu, Cong Liao, Jianguo Li, Weiyao Lin, Alex X Liu, and Schahram Dustdar. Pyraformer: Low-complexity pyramidal attention for long-range time series modeling and forecasting. In *Proceedings of the International Conference on Learning Representations*, 2021.
- [Salinas *et al.*, 2020] David Salinas, Valentin Flunkert, Jan Gasthaus, and Tim Januschowski. DeepAR: Probabilistic forecasting with autoregressive recurrent networks. *International Journal of Forecasting*, 36(3):1181–1191, 2020.
- [Sawhney *et al.*, 2021] Ramit Sawhney, Shivam Agarwal, Arnab Wadhwa, Tyler Derr, and Rajiv Ratn Shah. Stock selection via spatiotemporal hypergraph attention network: A learning to rank approach. In *Proceedings of the AAAI Conference on Artificial Intelligence*, pages 497–504, 2021.
- [Shabani *et al.*, 2022] Amin Shabani, Amir Abdi, Lili Meng, and Tristan Sylvain. Scaleformer: Iterative multi-scale refining transformers for time series forecasting. In *Proceedings of the International Conference on Learning Representations*, 2022.
- [Subramanian *et al.*, 2020] Sandeep Subramanian, Ronan Collobert, Marc’Aurelio Ranzato, and Y-Lan Boureau. Multi-scale transformer language models. *arXiv preprint arXiv:2005.00581*, 2020.

- [Taylor and Letham, 2018] Sean J Taylor and Benjamin Letham. Forecasting at scale. *The American Statistician*, 72(1):37–45, 2018.
- [Wang *et al.*, 2021] Wenhai Wang, Enze Xie, Xiang Li, Deng-Ping Fan, Kaitao Song, Ding Liang, Tong Lu, Ping Luo, and Ling Shao. Pyramid vision transformer: A versatile backbone for dense prediction without convolutions. In *Proceedings of the IEEE/CVF International Conference on Computer Vision*, pages 568–578, 2021.
- [Wen *et al.*, 2021] Qingsong Wen, Kai He, Liang Sun, Yingying Zhang, Min Ke, and Huan Xu. RobustPeriod: Robust time-frequency mining for multiple periodicity detection. In *Proceedings of the International Conference on Management of Data*, pages 2328–2337, 2021.
- [Wen *et al.*, 2022] Qingsong Wen, Tian Zhou, Chaoli Zhang, Weiqi Chen, Ziqing Ma, Junchi Yan, and Liang Sun. Transformers in time series: A survey. *arXiv preprint arXiv:2202.07125*, 2022.
- [Wu *et al.*, 2019] Zonghan Wu, Shirui Pan, Guodong Long, Jing Jiang, and Chengqi Zhang. Graph WaveNet for deep spatial-temporal graph modeling. In *Proceedings of the International Joint Conference on Artificial Intelligence*, pages 1907–1913, 2019.
- [Wu *et al.*, 2021] Haixu Wu, Jiehui Xu, Jianmin Wang, and Mingsheng Long. Autoformer: Decomposition transformers with auto-correlation for long-term series forecasting. *Advances in Neural Information Processing Systems*, pages 22419–22430, 2021.
- [Xia *et al.*, 2022] Lianghao Xia, Chao Huang, Yong Xu, Jia-shu Zhao, Dawei Yin, and Jimmy Huang. Hypergraph contrastive collaborative filtering. In *Proceedings of the International ACM SIGIR Conference on Research and Development in Information Retrieval*, pages 70–79, 2022.
- [Xu *et al.*, 2022] Chenxin Xu, Maosen Li, Zhenyang Ni, Ya Zhang, and Siheng Chen. GroupNet: Multiscale hypergraph neural networks for trajectory prediction with relational reasoning. In *Proceedings of the IEEE/CVF Conference on Computer Vision and Pattern Recognition*, pages 6498–6507, 2022.
- [Yadati *et al.*, 2019] Naganand Yadati, Madhav Nimishakavi, Prateek Yadav, Vikram Nitin, Anand Louis, and Partha Talukdar. HyperGCN: A new method for training graph convolutional networks on hypergraphs. *Advances in Neural Information Processing Systems*, pages 1–12, 2019.
- [Yan *et al.*, 2020] Yichao Yan, Jie Qin, Jiabin Chen, Li Liu, Fan Zhu, Ying Tai, and Ling Shao. Learning multi-granular hypergraphs for video-based person re-identification. In *Proceedings of the IEEE/CVF Conference on Computer Vision and Pattern Recognition*, pages 2899–2908, 2020.
- [Yang *et al.*, 2020] Dingqi Yang, Bingqing Qu, Jie Yang, and Philippe Cudré-Mauroux. LBSN2Vec++: Heterogeneous hypergraph embedding for location-based social networks. *IEEE Transactions on Knowledge and Data Engineering*, 34(4):1843–1855, 2020.
- [Yang *et al.*, 2022] Yuhao Yang, Chao Huang, Lianghao Xia, Yuxuan Liang, Yanwei Yu, and Chenliang Li. Multi-behavior hypergraph-enhanced transformer for sequential recommendation. In *Proceedings of the ACM SIGKDD Conference on Knowledge Discovery and Data Mining*, pages 2263–2274, 2022.
- [Zhang and Yan, 2023] Yunhao Zhang and Junchi Yan. Crossformer: Transformer utilizing cross-dimension dependency for multivariate time series forecasting. In *Proceedings of the International Conference on Learning Representations*, 2023.
- [Zhang *et al.*, 2021] Pengchuan Zhang, Xiyang Dai, Jianwei Yang, Bin Xiao, Lu Yuan, Lei Zhang, and Jianfeng Gao. Multi-scale vision longformer: A new vision transformer for high-resolution image encoding. In *Proceedings of the IEEE/CVF International Conference on Computer Vision*, pages 2998–3008, 2021.
- [Zhou *et al.*, 2021] Haoyi Zhou, Shanghang Zhang, Jieqi Peng, Shuai Zhang, Jianxin Li, Hui Xiong, and Wancai Zhang. Informer: Beyond efficient transformer for long sequence time-series forecasting. In *Proceedings of the AAAI Conference on Artificial Intelligence*, pages 11106–11115, 2021.
- [Zhou *et al.*, 2022] Tian Zhou, Ziqing Ma, Qingsong Wen, Xue Wang, Liang Sun, and Rong Jin. FEDformer: Frequency enhanced decomposed transformer for long-term series forecasting. In *Proceedings of the International Conference on Machine Learning*, pages 27268–27286, 2022.